

Unintentional carbide formation evidenced during high-vacuum magnetron sputtering of transition metal nitride thin films

Grzegorz Greczynski, S. Mraz, Lars Hultman and J. M. Schneider

Journal Article



N.B.: When citing this work, cite the original article.

Original Publication:

Grzegorz Greczynski, S. Mraz, Lars Hultman and J. M. Schneider, Unintentional carbide formation evidenced during high-vacuum magnetron sputtering of transition metal nitride thin films, *Applied Surface Science*, 2016. 385(), pp.356-359.

<http://dx.doi.org/10.1016/j.apsusc.2016.05.129>

Copyright: Elsevier

<http://www.elsevier.com/>

Postprint available at: Linköping University Electronic Press

<http://urn.kb.se/resolve?urn=urn:nbn:se:liu:diva-131492>



Unintentional carbide formation evidenced during high-vacuum magnetron sputtering of transition metal nitride thin films

G. Greczynski,^{1,2} S. Mráz,² L. Hultman,¹ J.M. Schneider²

¹*Thin Film Physics Division, Department of Physics (IFM), Linköping University, SE-581 83 Linköping, Sweden*

²*Materials Chemistry, RWTH Aachen University, Kopernikusstr. 10, D-52074 Aachen, Germany*

Carbide signatures are ubiquitous in the surface analyses of industrially sputter-deposited transition metal nitride thin films grown with carbon-less source materials in typical high-vacuum systems. We use high-energy-resolution photoelectron spectroscopy to reveal details of carbon temporal chemical state evolution, from carbide formed during film growth to adventitious carbon adsorbed upon contact with air. Using *in-situ* grown Al capping layers that protect the as-deposited transition metal nitride surfaces from oxidation, it is shown that the carbide forms during film growth rather than as a result of post deposition atmosphere exposure. The XPS signature of carbides is masked by the presence of adventitious carbon contamination, appearing as soon as samples are exposed to atmosphere, and eventually disappears after one week-long storage in lab atmosphere. The concentration of carbon assigned to carbide species varies from 0.28 at% for ZrN sample, to 0.25 and 0.11 at% for TiN and HfN, respectively. These findings are relevant for numerous applications, as unintentionally formed impurity phases may dramatically alter catalytic activity, charge transport and mechanical properties by offsetting the onset of thermally-induced phase transitions. Therefore, the chemical state of C impurities in PVD-grown films should be carefully investigated.

Keywords: XPS; surface chemistry; magnetron sputtering; carbon; titanium nitride

Transition metal (TM) nitride-based thin films with applications, ranging from protective layers on high-speed cutting tools^{1,2} to diffusion barriers in electronics,^{3,4,5} are typically grown by physical vapor deposition (PVD). Low homologous temperatures ($T_s/T_m < 0.3$, where T_s and T_m stand for the substrate and the melting temperature, respectively) together with extremely high cooling rates (on the order of 10^{13} K/s) during the vapour condensation on the film surface, result in growth conditions far from thermodynamic equilibrium.⁶ This allows for synthesis of metastable phases with unique properties which paves the ground for heavily researched field.⁷

The presence of carbon impurities is regularly confirmed during surface analysis by x-ray photoelectron spectroscopy (XPS) in binary and ternary transition metal nitride films grown by PVD techniques such as magnetron sputtering,^{8,9,10,11,12,13,14} or cathodic arc evaporation.^{15,16,17,18,19,20} Often this is attributed to the post deposition atmosphere exposure and labeled as adventitious carbon adsorbed at the surface and/or at grain boundaries, hence, excluded from the discussion of microstructure – property relationships of the as deposited thin films. C 1s core-level signal is only used (if at all) for binding energy (BE) scale calibration,^{9,12,13,17,19,20} and spectra are published only occasionally, typically with a rather poor signal-to-noise ratio that prevents complete chemical state identification. Here it is shown that in addition to adventitious carbon another previously overlooked carbon population exists.

Direct evidence for unintentional and, at the same time, unexpected carbide formation during high-vacuum (HV) growth of group IVb transition metal nitride thin films by magnetron sputtering is presented. Layers are deposited in Ar/N₂ atmosphere using typical industrial sputter-deposition system under process conditions that are commonly employed for nitride growth. High-energy-resolution XPS analyses combined with the *in-situ* Al-capping technique²¹ are used to trace the temporal evolution of C chemical state starting from film growth, through venting and air exposure, to storage in the lab atmosphere. The signature of

carbides formed during film growth is masked by the presence of adventitious carbon contamination, appearing as soon as samples are exposed to atmosphere, and eventually disappears after one week-long storage in lab atmosphere. Possible source of incorporated carbon during film growth is residual gas and/or target impurities. The reaction may be triggered by gas ion bombardment that leads to recoil implantation and forward sputtering of adsorbed C species. This finding is relevant for numerous applications, as even small amounts of foreign (unintentional) phases may dramatically alter catalytic activity, charge transport or even mechanical properties by offsetting the onset of thermally-induced phase transitions.

Polycrystalline TiN, ZrN, and HfN thin films are grown on Si(001) substrates biased at -60 V by reactive dc magnetron sputtering (DCMS) in typical HV magnetron sputtering system using rectangular 8.8×50 cm² targets (>99.9 at% pure, excluding Zr in the case of Hf target) and Ar/N₂ gas mixture with N₂ partial pressure $p_{N_2} = 5.8 \times 10^{-4}$ Torr (76 mPa). The total pressure during deposition is 3 mTorr (0.4 Pa), while the system base pressure p_b before and after the film growth is 2.3×10^{-6} Torr (0.3 mPa) and 1.5×10^{-7} Torr (0.02 mPa), respectively. The average target power during 25-min-long deposition is 4 kW resulting in film thickness of 1.2 μm. The substrate temperature is 430 °C and the venting temperature is 270 °C.

XPS spectra are acquired from TiN, ZrN, and HfN films in a Kratos Analytical instrument, with a base pressure of 1.1×10^{-9} Torr (1.5×10^{-7} Pa), using monochromatic Al K α radiation ($h\nu = 1486.6$ eV). All samples exhibit pronounced cut-off in the density of states near the Fermi level – the Fermi Edge (FE), which occurs within ± 0.03 eV within that of the sputter-cleaned Ag sample used for calibration. Thus, core-level spectra are referenced to the FE that defines “zero” on the BE scale. Deconvolution and quantification is performed using the CasaXPS software with elemental sensitivity factors supplied by Kratos Analytical Ltd.²²

Figure 1 shows C1s core level spectra acquired from TiN, ZrN, and HfN surfaces exposed to the ambient atmosphere for ~2 minutes necessary to transfer samples to the XPS

instrument. All spectra possess clear signature of four contributions corresponding to four chemical states of C atoms in the probed surface region. The three strongest peaks are due to adventitious carbon contamination: C-C/C-H (284.3-285.3 eV), C-O (286.0-287.1 eV), and O-C=O (288.7-289.7 eV). While the relative BE shifts between these three components are the same in all cases, the absolute values vary between the samples (e.g. C-C/C-H component is present at 284.3 eV for TiN and at 285.3 eV for ZrN film), which is the consequence of the fact that BE is not only set by the chemical environment but also the type of the underlying surface matters (in this case surface oxides with different conductivity). In addition to adventitious carbon there is also a clear contribution at significantly lower BE visible in all three cases, which is assigned to carbide formation. The position of this peak varies slightly from 282.1 eV for TiN to 282.2 and 282.4 eV for ZrN and HfN respectively.^{23,24,25} The magnitude of BE shift in the case of carbide peak (0.3 eV) is thus significantly smaller than that observed for adventitious carbon (1.0 eV) which indicates that carbide species are buried below the surface native oxide layer, i.e., formed during film growth, hence their BE is not affected by oxide conductivity. The concentration of carbon assigned to carbide species varies from 0.28 at% for ZrN sample, to 0.25 and 0.11 at% for TiN and HfN, respectively.

The angle-dependent XPS studies are used to reveal details of carbon chemical state evolution during film growth. Fig. 2(a) shows normalized C 1s spectra of TiN sample acquired at the photoelectron take-off angle ϕ of 90 and 10 degrees. In the latter case the probing depth is reduced by a factor of $1/\sin(\phi) = 5.7$, which has a pronounced effect on the relative peak intensities. The C-O and O-C=O components are drastically reduced with respect to C-C/C-H contribution, indicating that former species are located closer to the native oxide surface. The most striking difference, however, is the lack of carbide peak in the surface-sensitive spectrum. This reveals that Ti-C species are buried under the oxide layer, in agreement with the previous assessment of carbide formation during film growth, which is followed by C-O/O-C=O and C-

C/C-H buildup upon air exposure. The following stages of C chemical state evolution are mapped out in Figure 2(b), where the C 1s spectra recorded from TiN films as a function of air exposure time, from 2 to 10⁴ minutes (~1 week), are shown. The main effect is the accumulation of C-C/C-H-type carbon that eventually dominates the signal and leads to severe attenuation of the carbide signature which is barely detectable after one week. Thus, the here reported observation of carbide species was enabled by minimizing the air exposure time.

In order to exclude possibility that TiC forms upon contact with air rather than during film growth, an additional TiN layer is deposited and Al-capped *in-situ* in the deposition system prior to air-exposure. Recent studies showed that 15-Å-thick Al capping layer provides effective barrier to TiN sample oxidation.²¹ Here, we employ thicker capping, $d_{Al} = 56 \text{ \AA}$, (Ref.26) that is then *in-situ* thinned prior to XPS analyses²⁷ in order to remove adventitious C from the Al surface without affecting the TiN film. In this way the chemical state of carbon on the as-deposited TiN surface (prior to air exposure) can be directly accessed. Figure 3 shows (a) C 1s and (b) Al 2p spectra recorded from the Al/TiN sample (i) in the as-received state, (ii) with the *in-situ* thinned Al-cap, and (iii) with the Al-cap removed by longer (600 s) sputter etching. C 1s spectrum of the as-received film shows C-C/C-H and O-C=O components at 286.1 and 290.3 eV respectively, both due to adventitious C accommodated on the oxidized Al-cap surface. There is no signature of carbide formation in the Al-capping layer, which is explained by the getter effect of Ti resulting in 15× lower background pressure immediately after TiN growth. The Al 2p spectra from the as-received sample exhibits a strong broad peak at 75.8 eV corresponding to native Al-oxide²⁸ and a lower-intensity metallic Al peak at 72.9 eV.²⁹ Assuming the layer-over-layer Al-cap model and the inelastic mean free path for Al 2p electrons in both Al-metal and Al-oxide $\lambda = 28 \text{ \AA}$, (Ref. 30) the metal-to-oxide peak intensity ratio I_m/I_o can be expressed as

$$\frac{I_m}{I_o} = \frac{N_m}{N_o} \frac{(\exp[-d_o/\lambda] - \exp[-d_{Al}/\lambda])}{1 - \exp[-d_o/\lambda]}, \quad (1)$$

in which N_m and N_o are volume concentrations of Al atoms in metal and oxide layer and d_o is the Al-oxide thickness. Taking $N_m/N_o = 1.5$ for γ -Al₂O₃ (Ref. 31) and using $d_{Al} = 56$ Å determined in an independent measurement,²⁶ we can rewrite Eqn.(1) to express Al-oxide thickness as a function of I_m/I_o

$$d_o(\text{Å}) = 28 \ln \left[\frac{1+0.67I_m/I_o}{0.135+0.67I_m/I_o} \right]. \quad (2)$$

For the as-received Al/TiN sample Eqn.(2) gives $d_o = 41$ Å and, hence, the Al-metal thickness $d_m = 15$ Å.

The Al 2p spectrum obtained from Al/TiN sample with the *in-situ* thinned Al-cap shows significantly lowered intensity of the Al-oxide peak with respect to the Al-metal signal (see Fig. 3(b)). In this case Eqn.(2) yields $d_o = 27$ Å, hence the total Al-cap thickness is reduced to 42 Å after etching away part of the Al-oxide together with adventitious C layer. The thinned Al-capping layer has a larger thickness than the expected Ar⁺ ion penetration depth ξ determined by the effective extent of collision cascade events. The latter corresponds to the average Al-oxide primary recoil projected range and can be obtained from Monte Carlo simulations of ion/surface interactions.^{32,33} For Al and O recoils in the model γ -Al₂O₃ layer, $\xi_{Al} = 12$ Å and $\xi_O = 11$ Å with $E_{Ar^+} = 0.5$ keV and $\psi = 70^\circ$, hence $\xi < d_o$, *i.e.*, the *in-situ* thinning with 0.5 keV Ar⁺ ions is not expected to modify the underlying TiN surface.

Interestingly, the C 1s spectrum obtained after thinning the Al-capping layer possess very clear signatures of the carbide formation (see the inset in the upper panel of Fig. 3(a)) at 282.1 eV, *i.e.*, exactly the same BE as previously identified for the as-deposited TiN films (cf. Fig. 1). This peak stays intact and dominates C 1s signal once the Al-capping layer is completely removed after prolonged ion etch (cf. green curves in Figs. 3(a) and 3(b) representative of sputter-cleaned TiN surface). Thus, we can conclude that TiC is present in TiN films even if the atmosphere exposure is avoided.

It is beyond the scope of this letter to reveal the source of carbon contaminants that eventually lead to unintentional carbide formation. Under typical HV growth conditions employed in this work several sources of C are possible, with two perhaps most obvious choices being residual gas molecules and target contaminants. Dissociation of residual C=O molecules upon contact with TiN film surface can be expected based on the results of *ab initio* studies performed for the CO₂/TiAlN system.³⁴ In addition, C=O can dissociate upon electron impact in low pressure discharge (bond dissociation energy is 11.2 eV)³⁵ constituting alternative source of free carbon. Moreover, the apparently low level of target contaminants specified by the vendors (here < 0.1 %), can be misleading as light elements like C are preferably sputtered along the target normal,^{36,37} so their content in the film might be significantly higher than in the target, especially for lower values of pressure×distance product. Since both, the background system pressure and the target purity level used in this work are typical for industrial processing it is reasonable to assume that the unintentional carbide formation reported here for the growth of TiN, ZrN, and HfN, takes also place for other industrially-grown functional coatings with an affinity for carbon.

In conclusion, high-energy-resolution x-ray photoelectron spectroscopy analyses of group IVb transition metal nitride films grown by magnetron sputtering under typical industrial process conditions give direct evidence for the unintentional formation of carbides on the sub at.% level. By capping the freshly deposited films *in situ* we were able to trace the carbon chemical state evolution and show that carbide formation takes place during the film growth rather than upon air exposure. Our results show that the chemical state of C impurities in PVD-grown films should be carefully investigated.

The authors most gratefully acknowledge the financial support of the German Research Foundation (DFG) within SFB-TR 87, the VINN Excellence Center *Functional Nanoscale Materials* (FunMat) Grant 2005-02666, the Swedish Government Strategic Research Area in

Materials Science on Functional Materials at Linköping University (Faculty Grant SFO-Mat-LiU 2009-00971), and the Knut and Alice Wallenberg Foundation Grant 2011.0143.

Figure Captions

Fig. 1. C 1s XPS spectra obtained from as-received air-exposed (~2 min.) polycrystalline TiN, ZrN, and HfN thin films grown on Si(001) substrates by reactive DCMS in typical high-vacuum magnetron sputtering system at 430 °C. Arrows indicate the carbide component.

Fig. 2. (a) C 1s XPS spectra obtained from as-received air-exposed (~2 min.) polycrystalline TiN/ Si(001) sample at the electron take-off angle of 90° (black curve) and 10° (red curve); (b) C 1s XPS spectra obtained from polycrystalline TiN/Si(001) sample at the electron take-off angle of 90° as a function of air-exposure time.

Fig. 3. (a) C 1s and (b) Al 2p XPS spectra obtained from polycrystalline TiN/Si(001) sample capped *in-situ* with 56-Å-thick Al layer in the as-received state (black), with the Al-cap thickness reduced *in-situ* to 42 Å (red), and after complete removal of the Al-cap layer (green). Inset in panel (a) reveals details of the low-intensity C 1s spectra evolution.

REFERENCES

- ¹ O. Knotek, M. Böhmer, T. Leyendecker, *J. Vac. Sci. Technol. A* 4, 2695 (1986).
- ² T. Leyendecker, O. Lemmer, S. Esser, J. Ebberink, *Surf. Coat. Technol.* 48, 175 (1991).
- ³ M.-A. Nicolet, *Thin Solid Films* 52, 415 (1978).
- ⁴ I. Petrov, E. Mojab, F. Adibi, J.E. Greene, L. Hultman, J.-E. Sundgren, *J. Vac. Sci. Technol. A* 11, 11 (1993).
- ⁵ J.S. Chun, I. Petrov, J.E. Greene, *J. Appl. Phys.* 86, 3633 (1999).
- ⁶ See for instance: J.E. Greene, "Thin Film Nucleation, Growth, and Microstructural Evolution: an Atomic Scale View," in *Handbook of Deposition Technologies for Thin Films and Coatings*, Third Edition, ed. by P. Martin, William Andrew Publications (Elsevier), Burlington, MA (2010)
- ⁷ For review see: P. H. Mayrhofer, C. Mitterer, L. Hultman, H. Clemens, *Progress in Materials Science* 51 (2006) 1032; R. Hauert and J. Patscheider, *Advanced Engineering Materials* 2 (2000) 247
- ⁸ P.-Y. Jouan, M.-C. Peignon, Ch. Cardinaud and G. Lemperiere, *Applied Surface Science* 68 (1993) 595
- ⁹ J.J. Olaya, S.E. Rodil, S. Muhl, E. Sanchez, *Thin Solid Films* 474 (2005) 119
- ¹⁰ D. Schild, S. Ulrich, J. Ye, M. Stüber, *Solid State Sciences* 12 (2010) 1903
- ¹¹ H. Fager, G. Greczynski, J. Jensen, J. Lu, L. Hultman, *Surf. Coat. Technol.* 259 (2014) 442
- ¹² M. Futsuhara, K. Yoshioka, O. Takai, *Thin Solid Films* 322 (1998) 274
- ¹³ A. Mahmood, R. Machorro, S. Muhl, J. Heiras, F.F. Castillo, M.H. Farias, E. Andrade, *Diamond and Related Materials* 12 (2003) 1315
- ¹⁴ B. Subramanian, C.V. Muraleedharan, R. Ananthakumar, M. Jayachandran, *Surf. Coat. Technol.* 205 (2011) 5014
- ¹⁵ J.J. Nainaparampil, J.S. Zabinski, A. Korenyi-Both, *Thin Solid Films* 333 (1998) 88
- ¹⁶ A. Flink, M. Beckers, J. Sjöln, T. Larsson, S. Braun, L. Karlsson, L. Hultman, *J. Mater. Res.* 24/8 (2009) 2483
- ¹⁷ A. O. Eriksson, J. Q. Zhu, N. Ghafoor, J. Jensen, G. Greczynski, M. P. Johansson, Jacob Sjöln, M. Odén, L. Hultman, J. Rosén, *Journal of Materials Research* 26 (2011) 874-881
- ¹⁸ S.B. Sant, K.S. Gill, *Surf. Coat. Technol.* 68/69 (1994) 152
- ¹⁹ Y. Zhang, Y. Yang, Y. Zhai, P. Zhang, *Applied Surface Science* 258 (2012) 6897
- ²⁰ K. Dejun, F. Guizhong and W. Jinchuna, *Surf. Interface Anal.* 47 (2015) 198
- ²¹ G. Greczynski, I. Petrov, J.E. Greene, and L. Hultman, *J. Vac. Sci. Technol. A* 33 (2015) 05E101
- ²² Kratos Analytical Ltd.: library filename: "casaXPS_KratosAxis-F1s.lib"
- ²³ See Appendix E in "Surface Analysis by Auger and X-ray Photoelectron Spectroscopy" Ed. D. Briggs and J.T. Grant, IM Publications, Manchester, 2003.
- ²⁴ T. Zehnder, J. Patscheider, *Surface and Coatings Technology* 133-134 (2000) 138
- ²⁵ D. Craciun, G. Socol, N. Stefan, G. Bourne, V. Craciun, *Applied Surface Science* 255 (2009) 5260
- ²⁶ The exact thickness of the Al-cap layer is estimated from the attenuation of the Ti 2p and N 1s core levels
- ²⁷ In-situ thinning is performed by means of 30 s long sputter etch with low energy $E_{Ar^+} = 0.5$ keV Ar^+ ions and at the ion incidence angle $\psi = 70^\circ$ with respect to the surface normal.
- ²⁸ National Institute of Standards and Technology (NIST) X-ray Photoelectron Spectroscopy Database, Version 4.1 compiled by A.V. Naumkin, A. Kraut-Vass, S.W. Gaarenstroom, and C.J. Powell, <http://srdata.nist.gov/xps/> accessed on 2016-04-17
- ²⁹ J.F. Moulder, W.F. Stickle, P.E. Sobol, K.D. Bomben, "Handbook of X-ray Photoelectron Spectroscopy", Perkin-Elmer Corporation, Eden Prairie, USA, 1992
- ³⁰ S. Tanuma, C. J. Powell and D. R. Penn, *Surf. Interf. Anal.* 43 (2010) 689
- ³¹ B.R. Strohmeier, *Surf. Interf. Anal.* 15 (1990) 51
- ³² J. F. Ziegler, J. P. Biersack, U. Littmark, "The Stopping and Range of Ions in Solids," vol. 1 of series "Stopping and Ranges of Ions in Matter," Pergamon Press, New York (1984).
- ³³ www.srim.org; accessed on 2015-12-18.
- ³⁴ D. Music and J.M. Schneider, *New Journal of Physics* 15 (2013) 073004

³⁵ B. deB. Darwent, "National Standard Reference Data Series," National Bureau of Standards, No. 31, Washington, DC, 1970

³⁶ J. Neidhardt, S. Mráz, J. M. Schneider, E. Strub, W. Bohne, B. Liedke, W. Möller, and C. Mitterer, *J. Appl. Phys.* 104 (2008) 063304

³⁷ S. Mráz, J. Emmerlich, F. Weyand, and J. M Schneider, *J. Phys. D: Appl. Phys.* 46 (2013) 135501

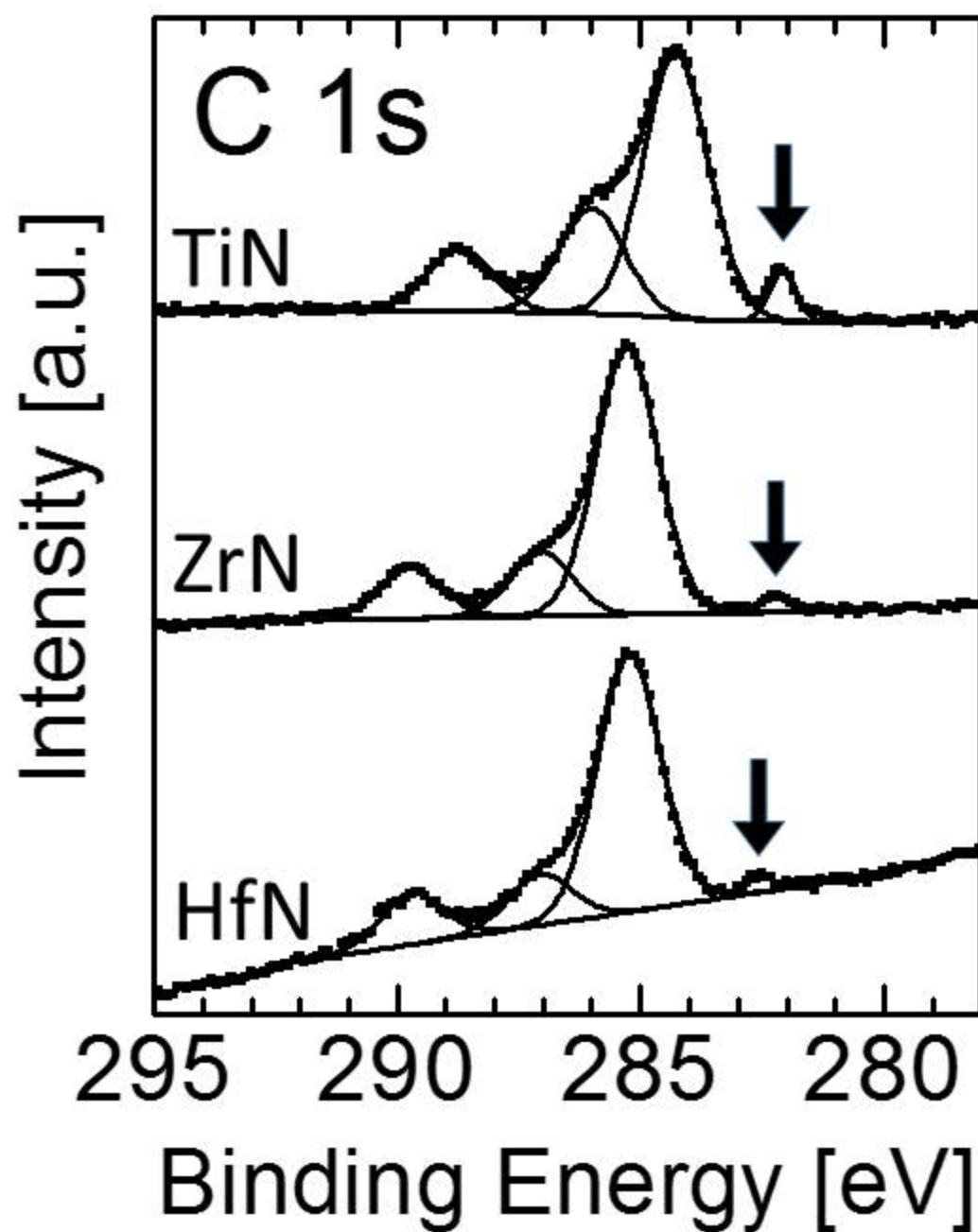


Fig. 1 C 1s XPS spectra obtained from as-received air-exposed (~2 min.) polycrystalline TiN, ZrN, and HfN thin films grown on Si(001) substrates by reactive DCMS in typical high-vacuum magnetron sputtering system at 430 °C. Arrows indicate the carbide component.

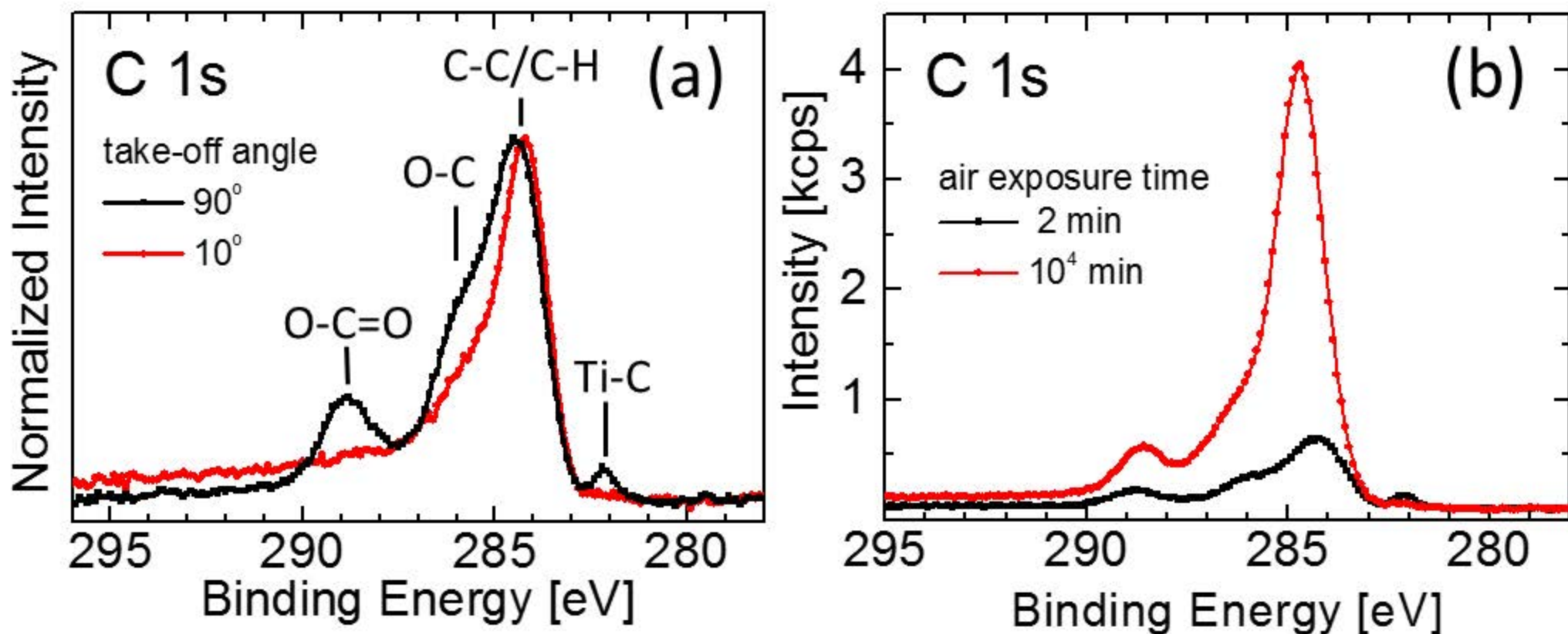


Fig. 2 (a) C 1s XPS spectra obtained from as-received air-exposed (~2 min.) polycrystalline TiN/Si(001) sample at the electron take-off angle of 90° (black curve) and 10° (red curve); (b) C 1s XPS spectra obtained from polycrystalline TiN/Si(001) sample at the electron take-off angle of 90° as a function of air-exposure time.

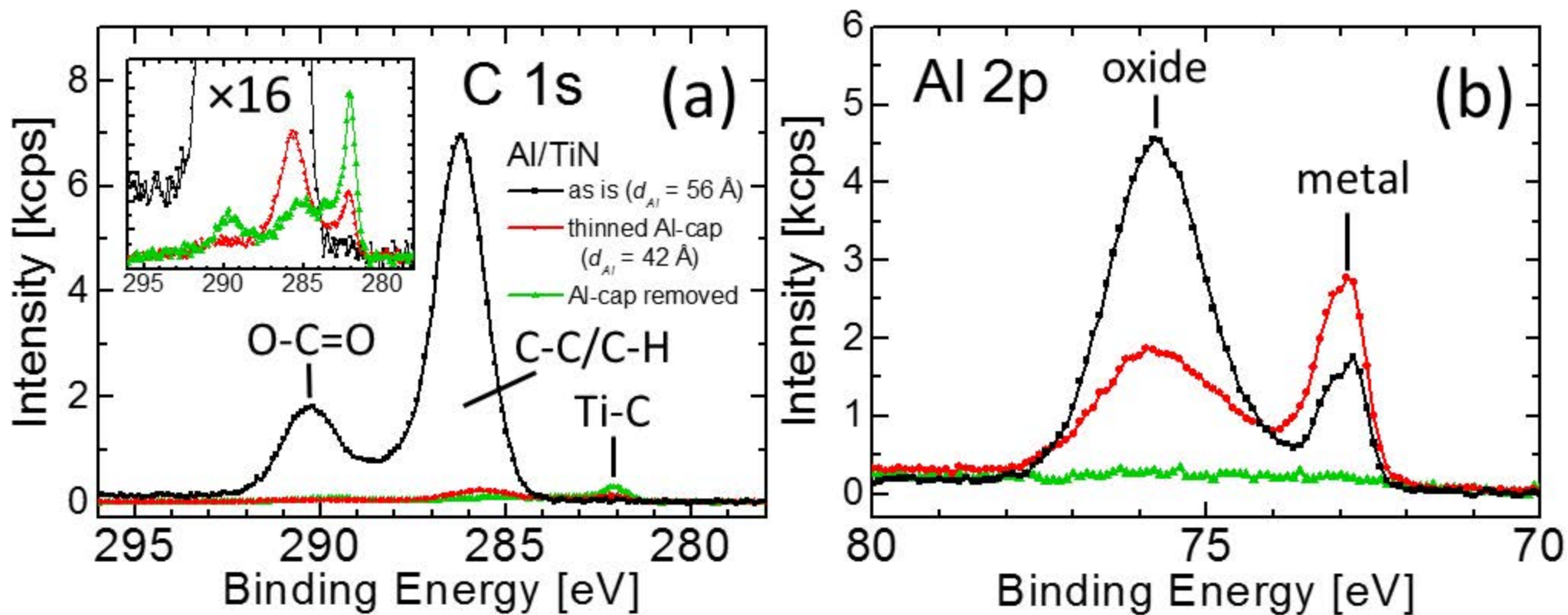


Fig. 3 (a) C 1s and (b) Al 2p XPS spectra obtained from polycrystalline TiN/Si(001) sample capped *in-situ* with 56-Å-thick Al layer in the as-received state (black), with the Al-cap thickness reduced *in-situ* to 42 Å (red), and after complete removal of the Al-cap layer (green). Inset in panel (a) reveals details of the low-intensity C 1s spectra evolution.